Article ID: 1000-7032(2018)04-0475-06

Structure Simulation and Vibration Spectra of $KTm_{0.1}Yb_{0.9}(WO_4)_2$ Laser Crystal

BI Lin[1*], DI Xiao-qiang[1], ZHAO Jian-ping[1], LI Chun[2], LIU Jing-he[2]

(1. *School of Computer Science and Technology, Changchun University of Science and Technology, Changchun* 130022, *China*;
2. *School of Materials Science and Engineering, Changchun University of Science and Technology, Changchun* 130022, *China*)

* *Corresponding Author, E-mail: bilin*7080@163.*com*

Abstract: $KTm_{0.1}Yb_{0.9}(WO_4)_2$ laser crystal was grown by the Kyropoulos method. The phase and structure of the crystal were studied using the X-ray single crystal diffraction and X-ray powder diffraction. Combined with the X-ray single crystal diffraction method, the structure model of the crystal was obtained by the diamond crystal graphics software. It is indicated that the crystal consists of WO_6, TmO_8/YbO_8 and KO_{12} groups. The W_2O_{10} dimers, which are connected by the single oxygen bridge(WOW), have a formation of the $(W_2O_8)_n$ multiple bands in the direction of parallel to the *c* axis. TmO_8/YbO_8 and KO_{12} are connected with the same vertex, which can form an extension band along the [101] and [110] directions with a two-dimensional structure. X-ray powder diffraction analysis indicates that the crystal belongs to monoclinic system with a space group *C*2/*c*. It is verified that as-grown crystal is β-double tungstate with low temperature. The cell parameters, crystal grain size and crystallinity of the crystal were calculated as well. The vibration spectra of the crystal were investigated. The vibration modes and frequencies of infrared and Raman peaks were identified, which could further verify the presence of WO_6 groups, single oxygen bridges(WOW) and double oxygen bridges(WOOW) in the crystal.

Key words: $KTm_{0.1}Yb_{0.9}(WO_4)_2$ laser crystal; structure simulation; vibration spectra
CLC number: O766; O482.31 **Document code**: A **DOI**: 10.3788/fgxb20183904.0475

掺铥钨酸镱钾激光晶体结构模拟及振动光谱

毕 琳[1*], 底晓强[1], 赵建平[1], 李 春[2], 刘景和[2]

(1. 长春理工大学 计算机科学技术学院, 吉林 长春 130022; 2. 长春理工大学 材料科学与工程学院, 吉林 长春 130022)

摘要: 采用泡生法生长了掺铥钨酸镱钾($KTm_{0.1}Yb_{0.9}(WO_4)_2$)激光晶体。利用X射线单晶衍射法和X射线粉末衍射法研究了 $KTm_{0.1}Yb_{0.9}(WO_4)_2$ 晶体的物相与结构。采用X射线单晶衍射法并结合 Diamond 晶体结构绘图软件,获得了晶体内部结构模型图:该晶体是由 WO_6、TmO_8/YbO_8和KO_{12}基团组成。W_2O_{10}二聚体通过 WOW 单氧桥相连,在平行于 *c* 轴方向上形成$(W_2O_8)_n$ 多重带。*Re*O_8 和 KO_{12}多面体共顶相连,沿[101]和[110]方向形成了具有二维层结构的延长带。X射线粉末衍射分析表明:该晶体具有低温β相双钨酸盐结构,属于单斜晶系,空间群 *C*2/*c*;计算了晶胞参数、晶粒尺寸和结晶度。测试了晶体的振动光谱,对各个峰值的红外和拉曼活性及分子振动情况进行了归属,进一步验证了晶体中 WO_6原子基团及单氧桥(WOW)和双氧桥(WOOW)的存在。

关 键 词: $KTm_{0.1}Yb_{0.9}(WO_4)_2$ 激光晶体; 结构模拟; 振动光谱

收稿日期: 2017-07-12; **修订日期**: 2017-09-20
基金项目: 吉林省科技发展计划(20160414043GH); 吉林省教育厅"十三五"科学技术研究项目(2016-379)资助
Supported by Jilin Provincial S&T Development Plan Project of China (20160414043GH); The 13th five-year S&T Research Project of Jilin Provincial Education Department of China(2016-379)

1 Introduction

In recent years, 2 μm solid-state lasers have been attracting much interest due to its widely potential applications, including eye-safe, laser remote sensing and laser medical treatment, *etc*[1-3]. Among the various of 2 μm solid-state laser mediums, Tm^{3+}-doped crystal has been of great interest since its broder gain spectrum in the region of 1.8 – 2 μm, as well as its long radiative lifetimes, which has been verified as a high efficiency and high-power laser source at 2 μm around[4-5].

$KR(WO_4)_2$ (R = Y and *Ln*) can be described as a laser host material with low symmetry, multi-wavelength and tunability, which belongs to the family of double tungstates[6-11], such as $KGd(WO_4)_2$, $KY(WO_4)_2$, $KYb(WO_4)_2$, *etc*. $KYb(WO_4)_2$ crystal has been included in the double tungstates family, with the $C2/c$ space group[12]. $KYb(WO_4)_2$ can be regarded as an excellent laser medium due to its advantages like high efficiency and high doping concentration, which is beneficial to producing super-speed pulse laser output[13-15].

In comparison of $KGd(WO_4)_2$ and $KY(WO_4)_2$ crystals, $KYb(WO_4)_2$ crystal has been one of more appropriate hosts to achieve high gain laser around 2 μm when doped with Tm^{3+}, Ho^{3+} ions, due to the high doping concentration of Yb^{3+} ions. This crystal can achieve all-solid-state, miniaturization and integration for lasers, which could be widely used in the fields of human-eye safe, laser communication, medical treatment, remote sensing, *etc*[16-19]. In this paper, the growth, structure simulation and vibration spectra of $KTm_{0.1}Yb_{0.9}(WO_4)_2$ laser crystal were studied.

2 Experiments

2.1 Crystal Growth

The chemicals were K_2CO_3 (Top-grade pure), Yb_2O_3 (99.99%), Tm_2O_3 (99.99%), and WO_3 (99.999%). The $K_2W_2O_7$ was chosen as solvent[20]. They were mixed and reacted as the equations below:

$$0.1Tm_2O_3 + 0.9Yb_2O_3 + K_2CO_3 + 4WO_3 \rightarrow 2KTm_{0.1}Yb_{0.9}(WO_4)_2 + CO_2\uparrow, \quad (1)$$

$$K_2CO_3 + 2WO_3 \rightarrow K_2W_2O_7 + CO_2\uparrow, \quad (2)$$

Where the mole ratio of $KTm_{0.1}Yb_{0.9}(WO_4)_2$ to $K_2W_2O_7$ was 1∶4.

The materials were put into an oven for 24 h to be sure they were fully dried, and then the materials were porphyrized and mixed evenly. The materials should be calcined beforehand so as to avoid volatilizing. The solvent $K_2W_2O_7$ was calcined until 600 ℃. The polycrystal raw material of $KTm_{0.1}Yb_{0.9}(WO_4)_2$ can be obtained when the calcination temperature was up to 920 ℃.

The experimental equipment mainly included a MCGE-Ⅲ furnace, a platinum crucible with a size of Φ60 mm × 50 mm, an AI-808P thermal controller and a P_t-R_h thermocouple. The $KTm_{0.1}Yb_{0.9}(WO_4)_2$ crystal was grown by the Kyropoulos method. The mixed materials was put in a platinum crucible and fully melted at a temperature of 80 ℃ above supersaturation for 24 h. Then an oriented seed was put into the melt when the temperature decreased to 5 ℃ above supersaturation. The crystal was gradually grown at a cooling rate of 0.1 ℃/h. Then the crystal was separated when the crystal growth process was end, and then it was cut to serve as the crystallon. When the oven temperature was decreased to 1 – 2 ℃ above supersaturation for 1 h, the crystallon was oriented. Then the growth continued at a rotation rate of 10 rad/min, a cooling rate of 0.05 ℃/h. After 2 weeks, the crystal was removed from the crucible and cooled down to the room temperature at a rate of 20 ℃/h. Eventually, the as-grown $KTm_{0.1}Yb_{0.9}(WO_4)_2$ crystal with a dimension of 25 mm × 15 mm × 11 mm was obtained successfully.

2.2 Measurement of Sample

The crystal structure was analyzed by X-Ray Single Crystal Diffractometer (Germany BRUKER AXS company) and X-ray Powder Diffractometer with a Rigaku D/max-rA revolving target XRD apparatus, using a Cu Kα ray (λ = 0.154 056 nm) as the radiant. The infrared spectrum of the crystal was measured by a Fourier conversion IR spectroscopy (Model FTS135, BIO-RAD Company). The Raman spectrum of the crystal was measured by a Raman

spectroscopy (MKI-1000, Renishaw Company, pumping source: Ar laser; wavelength: 488 nm; power: 500 mW; resolution: 1 cm^{-1}).

3 Results and Discussion

3.1 X-ray Single Crystal Diffraction Analysis

Combined with the structure information of $KTm_{0.1}Yb_{0.9}(WO_4)_2$ crystal by X-ray single crystal diffraction method, the Diamond software was used to produce crystal structure model (see Fig. 1 and Fig. 2). Fig. 1 shows the projection of $KTm_{0.1}Yb_{0.9}(WO_4)_2$ crystal structure along *a*, *b*, *c* and (111) directions, respectively. It is indicated that the WO_6 is a distorted octahedron, which could be produced through the coordination between 1 wolframium atom and 6 oxygen atoms. It is obviously noticed that the wolframium atoms take up the symmetric position of C1. A partial enlargement graph of WO_6 can be seen in Fig. 2(a). The W_2O_{10} dimmer can be formed through the connection among the double oxygen bridge WOOW based on the interaction among the wolframium atoms. The W_2O_{10} dimmers can also be connected by virtue of the single oxygen bridging bond WOW, and then form the $(W_2O_8)_n$ bands along *c* axis in parallel direction. Fig. 2(b) shows a partial enlargement graph of $(W_2O_8)_n$ which are connected by the same edges. It can be seen from Fig. 2(c), the TmO_8/YbO_8 are produced based on the coordination between 1 rare earth atom and 8 oxygen atoms. Fig. 2(d) shows a partial enlargement graph of KO_{12}, which is formed by the coordination between 1 potassium atom and 12 oxygen atoms. The rare earth atoms and potassium occupy C2 symmetric position together by the way of statistical distribution. The 12-coordinate polyhedrons KO_{12} and 8-coordinated polyhedrons TmO_8/YbO_8 are connected *via* common vertex and an elongated band was formed with the two dimensional layer structure along [101] and [110] directions. The elongated band takes up the framework fully composed of Tm^{3+}, Yb^{3+} and WO_6.

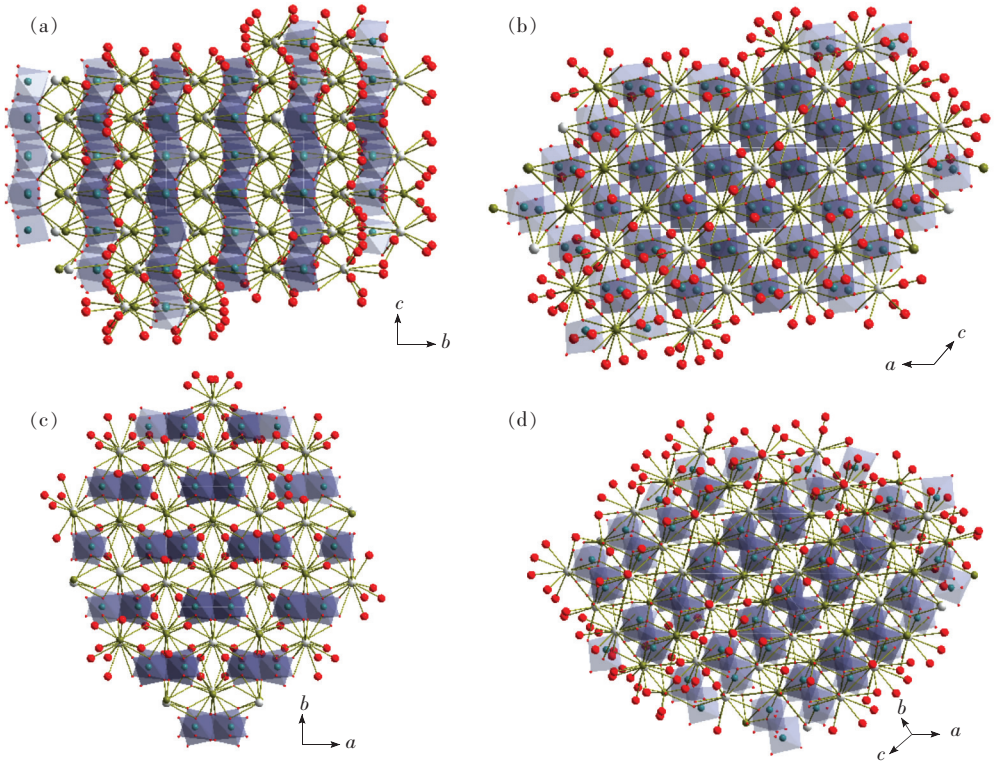

Fig. 1　Projection of $KTm_{0.1}Yb_{0.9}(WO_4)_2$ crystal structure along *a*, *b*, *c* and (111) directions. (a) Projection of $KTm_{0.1}Yb_{0.9}(WO_4)_2$ crystal structure along *a* axis. (b) Projection of $KTm_{0.1}Yb_{0.9}(WO_4)_2$ crystal structure along *b* axis. (c) Projection of $KTm_{0.1}Yb_{0.9}(WO_4)_2$ crystal structure along *c* axis. (d) Projection of $KTm_{0.1}Yb_{0.9}(WO_4)_2$ crystal structure along (111) direction.

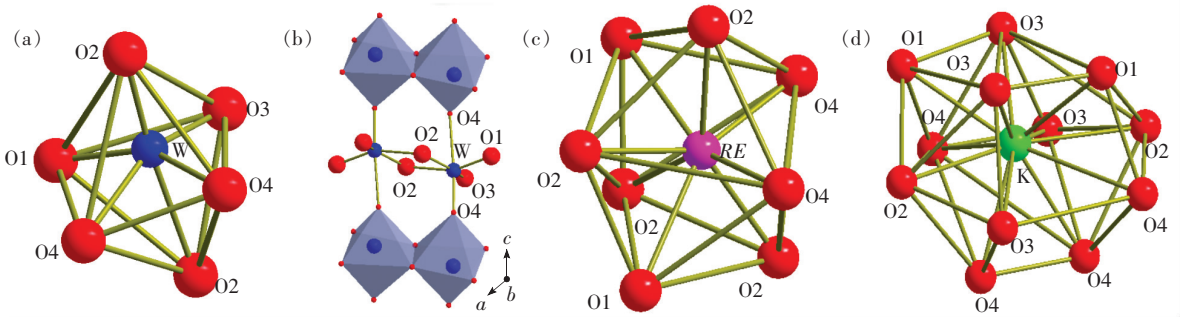

Fig. 2 Partial enlargement of WO_6, $(W_2O_8)_n$, TmO_8/YbO_8 and KO_{12}. (a) Partial enlargement of WO_6 distorted octahedron. (b) Partial enlargement of $(W_2O_8)_n$ bands. (c) Partial enlargement of REO_8 (RE = Tm/Yb) polyhedrons. (d) Partial enlargement of KO_{12} polyhedrons.

3.2 X-ray Powder Diffraction Analysis

The X-ray powder diffraction pattern of $KTm_{0.1}Yb_{0.9}(WO_4)_2$ crystal is shown in Fig. 3, and the peaks of this crystal were assigned accordingly. The diffraction spectrum shows that the diffraction peaks and relative intensity of the crystal are very similar to those of β-KYW, compared with the JCPDS card No. 73-0057. Hence the crystal has a monoclinic phase with a space group $C2/c$. It is demonstrated that the as-grown crystal belongs to β-$KTm_{0.1}Yb_{0.9}(WO_4)_2$.

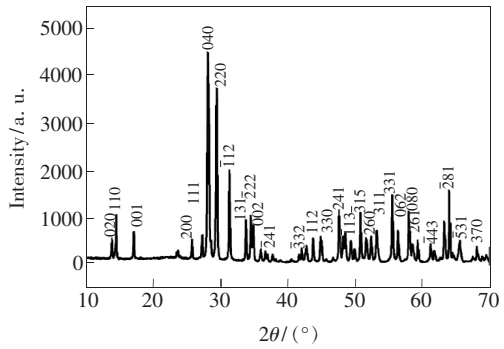

Fig. 3 X-ray power diffraction patterns of $KTm_{0.1}Yb_{0.9}(WO_4)_2$ crystal

According to Equation (3), the cell parameters of the crystal can be calculated as $a = 1.064$ nm, $b = 1.032$ nm, $c = 0.752$ nm, $\beta = 130.65°$, $Z = 4$.

$$d = \frac{ABC\sin\beta}{\sqrt{A^2B^2 + B^2C^2 + A^2C^2\sin^2\beta - 2AB^2C\cos\beta}}, \quad (3)$$

where A, B, C represent the intercept of the crystal plane whose distance is the minimum on a, b, c axes, and the distance is from the (hkl) family of crystal planes to the original point, where $A = a/h$, $B = b/k$, $C = c/l$. The crystal grain size and crystallinity of the crystal are also calculated using X-ray power diffraction analysis software as 35.3 – 116.2 nm and 92.36%, respectively.

3.3 Vibrational Spectra Analysis

It can be seen from Fig. 4 that the infrared absorption peak of the crystal at 474 cm^{-1} indicates the wagging vibration of WO_4 group, and the infrared absorption peaks at 636, 771, 840, 889, 926 cm^{-1} can be attributed to the stretching vibration of WO_4 group. When the sample was placed in the air, some water came into the sample, so the infrared

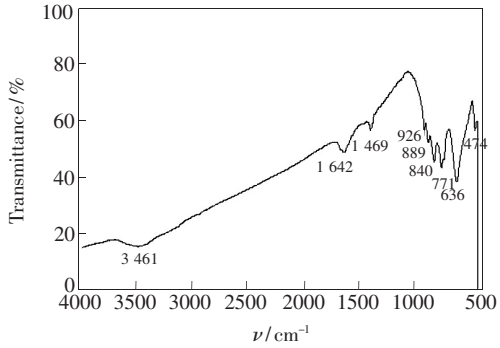

Fig. 4 Infrared spectrum of $KTm_{0.1}Yb_{0.9}(WO_4)_2$ crystal

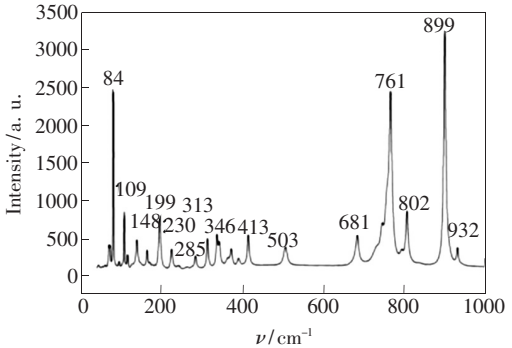

Fig. 5 Raman spectra of $KTm_{0.1}Yb_{0.9}(WO_4)_2$ crystal

absorption peaks at 1 642 cm^{-1} (1 469 cm^{-1}) and 3 461 cm^{-1} are due to the bending vibration and asymmetric stretching of the O—H bond. The Raman spectrum of the crystal can be seen in Fig. 5. The stronger Raman peaks at 84, 109, 199, 346, 413, 681, 761, 802, 899 cm^{-1} and the weaker red light at 650 nm were observed, which indicates the crystal has multiple bonds with high-covalency. Tab. 1 lists the vibration frequencies assignment of the crystal as for IR and Raman spectra. The results demonstrate the existence of the double oxygen bridge (WOOW) and the single oxygen bridge (WOW) in the crystal.

Tab. 1　Assignment of IR and Raman spectra in $KTm_{0.1}Yb_{0.9}(WO_4)_2$ crystal

Assignment	$KTm_{0.1}Yb_{0.9}(WO_4)_2$	
	RS/cm^{-1}	IR/cm^{-1}
T(WO_6)	84	
	109	
L(K^+/Yb^{3+})	148	
	162	
L(WO_6)	199	
δ(WOW) bending	230	
δ(WOOW) out-of-plane bending	285	
δ_s(WO_6)	313	
	346	
	372	
δ_{as}(WO_6)	403	
δ(WOOW) in-plane bending	413	
ω(WOOW) out-of-plane wagging	503	474
v_s(WOW) stretching	681	636
v(WOOW) stretching	761	771
$v_{as}(WO_6) + v_{as}$(WOW)	802	840
$v_s(WO_6) + v$(WOOW)	899	889
v_s(WO_6)	932	926
δ_{as}(OH)		1 469
		1 642
v_{as}(OH)		3 461

4　Conclusion

$KTm_{0.1}Yb_{0.9}(WO_4)_2$ laser crystal was grown by the Kyropoulos method. The structure of the crystal was investigated through the X-ray single crystal diffraction. The structure model of the crystal was obtained using the Diamond crystal graphics software. The crystal structure is composed of WO_6, TmO_8/YbO_8 and KO_{12} groups. The W_2O_{10} dimers, which are connected by the single oxygen bridge (WOW), have a formation of the $(W_2O_8)_n$ multiple bands in the direction of parallel to the *c* axis. TmO_8/YbO_8 and KO_{12} are connected with the same vertex, which can form an extension band along the [101] and [110] directions with a two-dimensional structure. Powder X-ray diffraction analysis indicates that the crystal belongs to monoclinic crystal system with a space group *C*2/*c*. The cell parameters of the crystal calculated are $a = 1.064$ nm, $b = 1.032$ nm, $c = 0.752$ nm, $\beta = 130.65°$, $Z = 4$. The crystal grain size and crystallinity of the crystal are also calculated using X-ray power diffraction analysis software as 35.3 – 116.2 nm and 92.36%, respectively. The vibration spectra of the crystal were investigated, and the vibration modes and frequencies of infrared and Raman peaks were identified, which can demonstrate the existence of WO_6 group, single oxygen bridge (WOW) and double oxygen bridge (WOOW) in the crystal.

References:

[1] GAPONENKO M, KÜLESHOV N, SÜDMEYER T. Efficient diode-pumped Tm: KYW 1.9-μm microchip laser with 1 W cw output power [J]. *Opt. Express*, 2014, 22 (10): 11578.

[2] ZOU X, LENG Y X, LI Y Y, *et al.*. Passively *Q*-switched mode-locked Tm: LLF laser with a MoS_2 saturable absorber [J]. *Chin. Opt. Lett.*, 2015, 13(8): 081405.

[3] GAO W L, MA J, XIE G Q, *et al.*. Highly efficient 2 μm Tm: YAG ceramic laser [J]. *Opt. Lett.*, 2012, 37(6): 1076.

[4] LAGATSKY A A, CALVEZ S, GUPTA J A, *et al.*. Broadly tunable femtosecond mode-locking in a Tm: KYW laser near 2 μm [J]. *Opt. Express*, 2011, 19(10): 9995-10000.

[5] WANG Y, LAN J L, ZHOU Z Y, *et al.*. Continuous-wave laser operation of diode-pumped Tm-doped $Gd_3Ga_5O_{12}$ crystal [J]. *Opt. Mater.*, 2017, 66:185-188.

[6] KAMINSKII A A, KLEVTSOV P V, LI L, *et al.*. Stimulated emission of $KY(WO_4)_2$: Nd^{3+} crystal laser [J]. *Phys. Stat. Sol.*, 1971, A5:79-81.

[7] DEMIDOVICH A A, KUZMIN A N, NIKEENKO N K, *et al.*. Optical characterization of Yb, Tm: KYW crystal concerning laser application [J]. *J. Alloys Compd.*, 2002, 341(122):124-129.

[8] 牛荣莲, 刘成成, 刘莹, 等. 基于侧面热对流的 LD 泵浦 Yb:$KGd(WO_4)_2$ 热透镜效应研究 [J]. 光子学报, 2011, 40(1):78-82.
NIU R L, LIU C C, LIU Y, *et al.*. Thermal lensing effect of diode-pumped Yb: $KGd(WO_4)_2$ based on convective heat-transfer on the side surface [J]. *Acta Photon. Sinica*, 2011, 40(1):78-82. (in Chinese)

[9] YAO Q, ZHANG J Y, LI J, *et al.*. Growth and spectral properties of $KNd(WO_4)_2$ [J]. *Mater. Lett.*, 2016, 185: 260-263.

[10] 吴冬妮, 崔瑞瑞, 龚新勇, 等. 新型红色荧光粉 $NaLa_{0.7}(MoO_4)_{2-x}(WO4)_x$:$0.3Eu^{3+}$ 的制备及发光性质研究 [J]. 发光学报, 2016, 37(3):274-279.
WU D N, CUI R R, GONG X Y, *et al.*. Synthesis and photoluminescence properties of $NaLa_{0.7}(MoO_4)_{2-x}(WO4)_x$: $0.3Eu^{3+}$ novel red phosphors [J]. *Chin. J. Lumin.*, 2016, 37(3):274-279. (in Chinese)

[11] 骆永石, 张家骅, 张霞. 掺铒碲钨酸盐玻璃光谱性质的研究 [J]. 中国光学, 2009, 2(1):54-59.
LUO Y S, ZHANG J H, ZHANG X. spectroscopic properties of tungsten-tellurite glasses doped with Er^{3+} ions at different concentrations [J]. *Chin. Opt.*, 2009, 2(1):54-59. (in Chinese)

[12] PUJOL M C, MATEOS X, SOLÉ M A R, *et al.*. Structure, crystal growth and physical anisotropy of $KYb(WO_4)_2$, a new laser matrix [J]. *J. Appl. Cryst.*, 2002, 35:108-112.

[13] 李云青, 崔彩娥, 黄平, 等. Pr^{3+}, Yb^{3+} 双掺的 $CaWO_4$ 荧光粉的近红外量子剪裁 [J]. 光子学报, 2015, 44(7):0716001.
LI Y Q, CUI C E, HUANG P, *et al.*. Near infrared quantum cutting in Pr^{3+}, Yb^{3+} co-doped $CaWO_4$ phosphors [J]. *Acta Photon. Sinica*, 2015, 44(7):0716001. (in Chinese)

[14] BRENIER A. A new evaluation of Yb^{3+}-doped crystals for laser applications [J]. *J. Lumin.*, 2001, 92:199-201.

[15] KLOPP P, GRIEBNER U, PETROV V, *et al.*. Laser operation of the new stoichiometric crystal $KYb(WO_4)_2$ [J]. *Appl. Phys.* B, 2002, 74:185-189.

[16] PUJOL M C, BURSUKOVA M A, GÜELL F, *et al.*. Growth, optical characterization, and laser operation of a stoichiometric crystal $KYb(WO_4)_2$ [J]. *Phys. Rev.* B, 2002, 65(16):160322.

[17] MATEOS X, PUJOL M C, GÜELL F, *et al.*. Sensitization of Er^{3+} emission at 1.5 μm by Yb^{3+} in $KYb(WO_4)_2$ single crystals [J]. *Phys. Rev.* B, 2002, 66(21):214104.

[18] LOIKO P, MATEOS X, DUNINA E, *et al.*. Judd-Ofelt modelling and stimulated-emission cross-sections for Tb^{3+} ions in monoclinic $KYb(WO_4)_2$ crystal [J]. *J. Lumin.*, 2017, 190:37-44.

[19] LOIKO P A, VILEJSHIKOVA E V, MATEOS X, *et al.*. Europium doping in monoclinic $KYb(WO_4)_2$ crystal [J]. *J. Lumin.*, 2017, 183:217-225.

[20] SOLE R, NIKOLOV V, RUIZ X, *et al.*. Growth of β-$KGd_{1-x}Nd_x(WO_4)_2$ single crystals in $K_2W_2O_7$ solvents [J]. *J. Cryst. Growth*, 1996, 169:600-603.

毕琳(1984 -),女,吉林松原人,博士,讲师,2016 年于中国科学院大学获得博士学位,主要从事计算机应用、计算机模拟仿真等方面的研究。
E-mail: bilin7080@163.com